Bound polaron in a spherical quantum dot: The all-coupling variational approach

Dmitriy V. Melnikov and W. Beall Fowler
Physics Department and Sherman Fairchild Center, Lehigh University, Bethlehem, Pennsylvania 18015
(Received 17 January 2001; revised manuscript received 31 May 2001; published 30 October 2001)

The effect of the electron-phonon interaction on an electron bound to an impurity in a spherical quantum dot embedded in a nonpolar matrix is studied theoretically. The all-coupling variational method is used to calculate the polaron energy shift including interaction with both bulk and surface LO phonons. The interaction of an electron with the image charge potential is taken into account. Comparison with the results of the adiabatic approach is also provided. General analytical results are obtained for small and large dots for different impurity positions. Numerical studies of the polaron properties have been performed for quantum dots of different radii with arbitrary strengths of the electron-phonon coupling and electron-impurity binding. It is shown that (1) as a function of the impurity position, the total value of the electron-phonon interaction has a maximum (in magnitude) when the impurity is located in the center of the dot in the case of weak coupling, and reaches its maximum at some intermediate impurity position for greater values of the electron-phonon and electron-impurity interactions and; (2) as a function of the impurity position, the interaction with surface phonons is greater for strong binding when the impurity is close to the boundary of the dot, reaches a maximum when the impurity is positioned on the surface of the dot in the weak coupling case and at some arbitrary impurity position inside the dot for the strong electron-phonon coupling and/or binding.

DOI: 10.1103/PhysRevB.64.195335 PACS number(s): 73.21.La, 71.38.−k, 71.55.−i

I. INTRODUCTION

Progress in crystal growth techniques has made it possible to fabricate semiconductor nanostructures with characteristic dimensions of the order of the electron or hole de Broglie wavelength. In these systems electronic states are subject to a strong dimensional confinement effect arising from the mismatch in the band gaps of the constituent materials. Among various kinds of nanostructures (quantum wells and superlattices with electronic confinement in one dimension, quantum wires with two-dimensional confinement potentials, and quantum dots with the quantum confinement present in all three dimensions), quantum dot (QD) systems have attracted the most attention because of their potential applications to electronic and optoelectronic devices[1,2] and the interesting quantum-mechanical phenomena associated with them; e.g., exciton states remain stable at room temperature, and the so-called phonon bottleneck may exist under some conditions (an electron in the excited state cannot relax by virtue of phonon emission when the distance between electron levels is not equal to the phonon energy).

Electron-phonon coupling in nanostructures also has different features from that in the bulk. That is, there is a strong increase of its strength with the reduction of dimensionality [from three-dimensional (3D) in the bulk to 0D in the quantum dot]. In these confined systems the dielectric constants of the materials inside and outside the structure differ from each other, and the resulting surface optical (SO) modes[3] need to be considered. To discuss phonon effects on electrons in nanostructures in a proper way, these phonon features (polaron effects) have to be taken into account.

Since the QD is one of the simplest examples of quantum confined structures, the polaron effects on an electron have been studied extensively both theoretically and experimentally. Polaron effects have been studied theoretically in QD's of various forms: spherical QDs,[4–7] cylindrical QDs,[8] rectangular quantum boxes,[9] and QD's with a parabolic confinement potential.[10–13] In spherical quantum dots polaron effects have been investigated within the dielectric continuum model.[4,5] These effects were studied for the case of the a polaron in a spherical QD (an electron confined in a QD interacts with phonons) implementing an adiabatic approximation,[4–6] in which surface optical phonon modes do not contribute to the polaron energy shift. Second-order perturbation theory[14] was also used to calculate the polaron shift; it was found that bulk-type phonons play a dominant role in the polaron energy shift. The all-coupling variational technique,[7] valid for a wide range of dot radii and electron-phonon coupling strengths, was also developed, and systematic calculations of the polaron energy shift were performed. The major results of these considerations are that (1) bulk phonons play the most important role in the polaron effects and the contribution from the SO phonons is either negligible or nonexistent; and (2) with the increase of the dot's radius the magnitude of the polaron energy shift decreases rapidly from a large value and then gradually approaches its bulk value. Experimental studies of electron-phonon interaction in QD's were concerned mainly with the measurement of the effective value of the Huang-Rhys factor (see, e.g., Refs. 15 and 16, and references therein); the major observed result is the increase of its value with the decrease of the dot size for well-formed QD's.

The study of impurity states in nanostructures is also important, since the impurities greatly affect both electronic and optical properties of the real QD's, much as in the bulk case.[17] Since the impurity can be located, in principle, anywhere in the dot, it is necessary to study the dependence of all relevant physical quantities on its position. The problem of the polaron effect on the so-called donorlike exciton in nanocrystals can also be treated within the frameworks of models applied to the free polaron case.[6] A recent experimental study of the luminescence in AgCl nanocrystals[18] in-

TABLE I. Values of the material parameters for typical semiconductor QD's: m_e, electron effective mass (in units of the free electron mass); $\hbar\omega_{LO}$, LO-phonon frequency (in meV); ε_0, static dielectric constant; ε_∞, high-frequency dielectric constant; α, electron-phonon coupling constant. Values of these parameters are taken from Ref. 24 for InAs and PbS, Ref. 25 for GaN, Ref. 23 for ZnSe, and Ref. 7 for all other materials.

	InAs	GaAs	GaN	CdSe	CuCl	ZnS	ZnSe	TlCl	KBr	PbS
m_e	0.0239	0.067	0.2	0.13	0.504	0.34	0.171	0.424	0.369	0.08
$\hbar\omega_{LO}$	29.63	35.33	92.5	26.54	25.64	43.18	38.49	21.46	20.97	25.4
ε_0	15.2	12.4	9.8	9.3	7.9	8	8.33	4.76	4.52	169
ε_∞	12.3	10.6	5.4	6.1	3.61	5.1	5.9	2.94	2.39	17.2
α	0.05	0.07	0.45	0.46	2.46	0.74	0.38	2.94	3.05	0.34

dicated that the compact, heavy hole can be trapped at different lattice sites, causing changes in peak positions in the observed spectra when it tunnels or hops toward the center of the nanocrystal.

The binding energy of the electron in a spherical QD was also studied[6,19–23] theoretically. In Refs. 19–21 the dependence of the binding energy for the ground state and several excited electronic states on the location of the impurity was investigated by means of variational calculations. It was found, in particular, that the binding energy of the ground state has a maximum when the impurity is positioned at the center of the dot, and that it decreases with a shift of the impurity from the center. In Refs. 22 and 23 the influence of electron-phonon interaction on that energy was investigated in the adiabatic case, varying the impurity position and the radius of the QD, and it was shown, in particular, that unlike a free polaron in a QD, the bound polaron interacts strongly with SO modes, especially when the impurity is located close to the dot's boundary.

In the present work we also study the effect of the electron-phonon interaction in a spherical QD for the case of an electron bound to a hydrogen like impurity (or donor like exciton with a heavy hole) located at some point within the dot. From the values presented in Table I, one can conclude that the material parameters of typical semiconductor QD's correspond to weak or intermediate electron-phonon coupling, which cannot be handled, generally speaking, by the adiabatic method. Thus, in this paper, calculations and discussion of the polaron energy shift are conducted for various values of the electron-phonon coupling and electron-impurity binding using the all-coupling variational approach similar to that from Ref. 7 in order to clarify the nature of the bound polaron confined in the spherical QD. The calculation of the polaron ground state (GS) energy is performed within the framework of the effective-mass approximation, i.e., assuming that all characteristic lengths of the problem are large compared to the lattice constant.[19]

This paper is organized in the following way. In Sec. II the all-coupling variational model for an electron in a spherical QD interacting with bulk and SO phonons is described. In Sec. III the general behavior of the bound polaron in small and large QD's is analyzed analytically. Special attention is paid to the cases when the impurity is located in the center of the dot or close to its boundary. Then, in Sec. IV the dependence of the polaron energy and electron-phonon interaction energies on the impurity position are studied numerically for different sizes of QD's using various values of electron-phonon and electron-impurity interactions and surrounding matrix material parameters. Finally, Sec. V gives the concluding remarks and outlines briefly possible future extensions of this model.

II. MODEL

Variational procedure

In this section, the basic equation that will be employed in the study of the bound polaron confined in the quantum dot is derived. This will be achieved by implementing the variational procedure to find the minimum expectation energy from the Hamiltonian of Ref. 23.

First, as is usually done for a bulk bound polaron, we eliminate the contribution to the total electron energy from the impurity–LO-phonon interaction. Next we implement the generalized Lee-Low-Pines theory first used to treat the exciton polaron problem,[26] generalized to the case of the bound bulk polaron,[27] and recently adapted for the case of a polaron confined in a spherical QD,[7] utilizing the unitary transformation

$$U=\exp\left\{\sum_{j,s}\left[F_{js}^{*}(\mathbf{r})a_{js}-F_{js}(\mathbf{r})a_{js}^{\dagger}\right]\right\}, \tag{1}$$

where parameters $F_{js}(\mathbf{r})$ are assumed to be real and are to be determined variationally. With these transformations taken into account, the trial wave function of the system is given by the product

$$|\Psi\rangle=U|\psi(\mathbf{r})\rangle|0\rangle, \tag{2}$$

where $|0\rangle$ is the phonon vacuum state.

Then the expectation value of the Hamiltonian[23] is given by

$$E=\langle\Psi|H|\Psi\rangle=\langle\psi|H_0|\psi\rangle, \tag{3}$$

where H_0 is the zero-phonon term of the transformed Hamiltonian $U^{-1}HU$:

$$H_0=\frac{\mathbf{p}^2}{2m}+V_{QD}(\mathbf{r})+V_C(\mathbf{r},\mathbf{r_0})+\sum_{j,s}\frac{\hbar^2}{2m}|\nabla F_{js}|^2$$
$$+\sum_{j,s}\hbar\omega_{js}|F_{js}|^2-\sum_{j,s}\hbar\omega_{js}[V_{js}S_{js}F_{js}+\text{H.c.}]. \tag{4}$$

The function $F_{js}(\mathbf{r})$ is taken in the following form:

$$F_{js}(\mathbf{r}) = V_{js} f_{js} + V_{js} S_{js}^{*}(\mathbf{r}) g_{js}. \tag{5}$$

The first term in this equation corresponds to the adiabatic method,[23] while the choice of the second one is appropriate to the intermediate electron-phonon coupling case. Note that in large QD's, the adiabatic approach is valid only for the strong electron-phonon and/or electron-impurity interactions. To describe weakly coupled or bound electrons in large quantum dots, it is necessary to use the intermediate-coupling variational approach. Thus it is expected that the form of F_{js} given by Eq. (5) will yield a reasonable description of the polaron effects for a wide range of the QD radii, electron-phonon, and electron-impurity interactions.

The subsequent minimization of Eq. (3) with respect to the variational parameters f_{js} and g_{js} leads to the following expressions for them:

$$f_{js} = \frac{A_{js} C_{js}}{B_{js} + C_{js} - A_{js}^2}, \tag{6}$$

$$g_{js} = \frac{B_{js} - A_{js}^2}{B_{js} + C_{js} - A_{js}^2}, \tag{7}$$

with coefficients A_{js}, B_{js}, and C_{js} defined by

$$A_{js} = \langle \psi | S_{js}(\mathbf{r}) | \psi \rangle, \tag{8}$$

$$B_{js} = \langle \psi | | S_{js}(\mathbf{r}) |^2 | \psi \rangle, \tag{9}$$

$$C_{js} = \frac{\hbar}{2 m^{*} \omega_{js}} \langle \psi | | \nabla S_{js}(\mathbf{r}) |^2 | \psi \rangle. \tag{10}$$

Choosing the electronic part of the trial function as a product of a ground-state wave function pertinent to the bare electron confined in the QD, and an exponential function describing the effect of the electron binding,

$$| \psi(\mathbf{r}) \rangle = N j_0 \left(\frac{\pi r}{R} \right) e^{-\gamma |\mathbf{r} - \mathbf{r}_0|}, \tag{11}$$

with N as a normalization constant and γ as a variational parameter indicating the degree of the spatial correlation between the electron and the impurity, after some calculations we can find E as a functional of the variational parameter γ:

$$E[\gamma] = \langle \psi | H_e + H_x | \psi \rangle + E_{pol}^{(b)} + E_{pol}^{(s)}, \tag{12}$$

where the electron–bulk-phonon ($E^{(b)}$) and electron–SO-phonon ($E^{(s)}$) interactions can be written in the following forms:

$$E_{pol}^{(b)} = -\sum_{s} \hbar \omega_{LO} V_{1s}^2 \left[A_{1s}^2 + \frac{(B_{1s} - A_{1s}^2)^2}{B_{1s} + C_{1s} - A_{1s}^2} \right], \tag{13}$$

$$E_{pol}^{(s)} = -\sum_{s} \hbar \omega_{l} V_{2s}^2 \left[A_{2s}^2 + \frac{(B_{2s} - A_{2s}^2)^2}{B_{2s} + C_{2s} - A_{2s}^2} \right]. \tag{14}$$

In the above expressions for the electron-phonon interaction energies, the first terms in brackets are the same as were obtained earlier for the adiabatic treatment of the polaron problem in the QD's.[6,23] The second parts can be interpreted as nonadiabatic contributions arising from the term in the function F_{js} dependent on the electron coordinate.

The energy of the bound polaron can be found by minimizing E with respect to the parameter γ. In the following calculations we will pay special attention to these quantities: the binding energy of the polaron, which is determined as a difference between the total energy of the polaron and the ground-state energy of the electron confined in the ''empty'' QD without the impurity present,

$$E_{tot} = E - \frac{\hbar^2}{2m} \left(\frac{\pi}{R} \right)^2, \tag{15}$$

and contributions to the total energy from electron–bulk-phonon ($E^{(b)}$) and electron–SO-phonon ($E^{(s)}$) interactions given by Eqs. (13) and (14).

III. ANALYTICAL RESULTS FOR LARGE AND SMALL QUANTUM DOTS

A. Polaron effects in the small quantum dot

Before proceeding with the numerical calculations of the polaron energy shift, it is interesting to find an analytical solution of Eqs. (12)–(14) in some limiting cases. This analytical consideration can be performed separately for the cases of the large and small QD's.

Let us first consider the case of a small QD with $R \ll a_B$, where a_B is the Bohr radius of the effective-mass electron. In this case the kinetic energy of the electron will predominate, and the interaction energy may be regarded as a perturbation to the free moving electron in the QD. This indicates that in order to obtain the leading term of the energy E_0, we can put $\gamma = 0$ in the electronic wave function [Eq. (11)], thus making it the eigenfunction of the unperturbed Hamiltonian. After some calculations, the final result for this term in the polaron binding energy can be cast in the form

$$E_0 = E_{C0} - E_{x0} + E_0^{(b)} + E_0^{(s)}, \tag{16}$$

where the E_{C0} representing the potential energy of the electron in the QD, the ''exchange'' energy E_{x0}, and the bulk $E_0^{(b)}$ and interface $E_0^{(s)}$ phonon intractions are equal to

$$E_{C0} = \frac{e^2}{\varepsilon_\infty R} \left[F\left(\frac{2\pi r_0}{R} \right) + \frac{1}{2} \left(\frac{\varepsilon_\infty}{\varepsilon_d} - 1 \right) - \frac{\varepsilon_\infty}{2} \sum_{l=1}^{\infty} \frac{\alpha_l}{\pi^{2l+1}} \int_0^{\pi} dx \sin^2(x) x^{2l} \right], \tag{17}$$

$$E_{x0} = \frac{e^2}{\varepsilon^{*} R} \left[F\left(\frac{2\pi r_0}{R} \right) - 1 \right], \tag{18}$$

$$E_0^{(b)} = -C_1 \frac{\alpha R_p}{R} \hbar\omega_{LO}, \tag{19}$$

$$E_0^{(s)} = -C_2 \frac{\alpha R}{R_p} \left(\frac{\varepsilon_0 \varepsilon_\infty^3}{(\varepsilon_0 + 2\varepsilon_d)(\varepsilon_\infty + 2\varepsilon_d)^3} \right)^{1/2} \hbar\omega_{LO}, \tag{20}$$

with the function $F(x)$ given by

$$F(x) = 1 - \frac{\sin(x)}{x} + \mathrm{cin}(2\pi) - \mathrm{cin}(x). \tag{21}$$

The coefficients $C_1 = [1 - \mathrm{Si}(2\pi) + \mathrm{Si}(4\pi)/2] = 0.7862$ and $C_2 = 4/3\pi^2\,(\pi^3/6 - \pi/4)^2 = 0.0266$, and $\mathrm{cin}(x)$ and $\mathrm{Si}(x)$ are the integral cosine and sine functions, respectively. In order to obtain Eqs. (18) and (19) above, first the summation over the roots of $j_0(x)$ was performed and then the resulting two-dimensional integrals were evaluated. Equation (20) was calculated using only the first term in the summation in Eq. (14) with $l=1$, and taking the limit of $R \ll R_p$, which can be justified by noting that in a small QD the distance between adjacent levels is large enough to provide a negligible mixing between states with higher values of l and the ground state.

The major difference between these results and those given in Ref. 23 for the adiabatic case is in the electron–SO-phonon interaction energy: unlike the adiabatic result, this energy is not equal to zero when the impurity located in the center of the QD. The value of $E_0^{(s)}$ is linearly proportional to the radius of the dot and will approach zero value only for $R \to 0$ when the adiabatic effects predominate. This indicates that this behavior of the electron–SO-phonon interaction is due to the presence of the nonadiabatic processes in the system, and thus cannot be obtained from the strong-coupling approach. The results and conclusions for the situation when $r_0 \to R$ are the same as given in Ref. 23, and will not be repeated here.

B. Electron-phonon coupling in a large quantum dot

The transition of the electronic state with the displacement of the impurity away from the surface of the dot becomes especially interesting when the dot's size becomes very large. Then we may expect to obtain the standard bulk bound polaron results when the impurity is in the center of the QD, and the bound surface polaron model will be appropriate to describe the impurity on the boundary of the dot. Let us first consider the case of an impurity in the center of the QD.

1. Impurity is in the center of the QD

Provided that the radius of the electron localization is much smaller than the dot's radius, the electronic wave function [Eq. (11)] is easily reduced to the form usually adopted for the description of the GS of the bulk bound polaron:[28]

$$|\psi(\mathbf{r})\rangle = \left(\frac{\gamma^3}{\pi} \right)^{1/2} e^{-\gamma \mathbf{r}}. \tag{22}$$

Using this wave function, the matrix elements A_{js}, B_{js}, and C_{js} can be presented in the forms

$$A_{1s} = \frac{1}{\sqrt{4\pi}} \delta_{l0} \langle \psi | e^{i\mathbf{k}\cdot\mathbf{r}} | \psi \rangle, \tag{23}$$

$$B_{1s} = \frac{1}{4\pi} \delta_{l0}, \tag{24}$$

$$C_{1s} = k^2 R_p^2 B_{1s}, \tag{25}$$

where δ_{l0} is Kronecker delta symbol, $k = \mu_{nl}/R$, and coefficients A_{2s}, B_{2s}, and C_{2s} approach zero. The fact that only the terms with $l=0$ have nonzero values can be explained by noting that in this case the trial wave function has a spherical symmetry (the electron is in the $1s$ state), and thus the corresponding intergrals give the most significant input to the total polaron energy shift.

After this, changing the summation over n in Eq. (13) into an integral over k gives rise to the following expression for $E_p^{(b)}$ in the large dot limit:

$$E_p^{(b)} = -\hbar\omega_{LO} \frac{2\alpha R_p}{\pi} \int_0^\infty dk \frac{1 - G_k^2 + R_p^2 k^2 G_k^2}{1 - G_k^2 + R_p^2 k^2}, \tag{26}$$

with $G_k = \langle \psi | e^{i\mathbf{k}\cdot\mathbf{r}} | \psi \rangle$. This is exactly the same equation as obtained by Matsuura and Büttner[26] for the case of the bound polaron in the bulk. The total polaron energy functional then takes the form

$$E[\gamma] = \frac{\hbar^2}{2m} \frac{\gamma^2}{4} - \frac{e^2}{\varepsilon_0} \frac{\gamma}{2} + E_p^{(b)}. \tag{27}$$

Using this expression the limiting cases of the weak binding and coupling ($G_{\mathbf{k}} \to 0$) and the strong binding and/or coupling (adiabatic approach, $G_k \to 1$ for most values of k)[17] can be easily obtained:

$$E[\gamma] = \frac{\hbar^2}{2m} \frac{\gamma^2}{4} - \frac{e^2}{\varepsilon_0} \frac{\gamma}{2} - \alpha\hbar\omega_{LO}, \tag{28}$$

$$E[\gamma] = \frac{\hbar^2}{2m} \frac{\gamma^2}{4} - \frac{e^2}{\varepsilon_0} \frac{\gamma}{2} - \frac{5}{16} \frac{e^2}{\varepsilon^*} \frac{\gamma}{2}. \tag{29}$$

Minimization of these equations with respect to the parameter γ immediately leads to the polaron energy E and the electron-phonon interaction energy $E_p^{(b)}$, given by

$$E = -\alpha\hbar\omega_{LO} - \frac{me^4}{2\hbar^2\varepsilon_0^2}, \quad E = -\frac{me^4}{2\hbar^2\varepsilon_0^2} \left[1 + \frac{5}{16} \frac{\varepsilon_0}{\varepsilon^*} \right]^2,$$

$$E_p^{(b)} = -\alpha\hbar\omega_{LO}, \quad E_p^{(b)} = -\frac{5}{16} \frac{me^4}{2\hbar^2\varepsilon_0\varepsilon^*} \left[1 + \frac{5}{8} \frac{\varepsilon_0}{8\varepsilon^*} \right], \tag{30}$$

which are the well-known expressions for the system with weak (left pair) and strong (right pair) electron-phonon coupling or binding in the bulk,[28] with the bare electron in the $1s$-state.

2. Impurity is on the surface of the QD

In this situation the electron will be localized around an impurity far away from the center of the dot. In order to simplify consideration in this case, a new coordinate system with an origin at the impurity position is introduced. Assuming that the radius of the electron localization is much smaller than the dot's size, one can cast the electron wave function [Eq. (11)] in the form

$$\psi(\mathbf{r})=\left(\frac{2\gamma^5}{\pi}\right)^{1/2} z e^{-\gamma\rho}, \tag{31}$$

where $z=\rho\cos\Theta$, and ρ and Θ are the radius and azimuthal angle in this new coordinate system. This is the wave function of the $2p$ state, which is appropriate for a description of the GS of the electron bound to the hydrogenlike impurity on the surface of the crystal.[29] One would expect that in this limit the results of the surface polaron theory should be recovered,[31] where interaction energies with both bulk and SO phonons make nonzero contributions to the total polaron energy.

Since we assumed that $r\gg\gamma^{-1}$, the asymptotic forms of the spherical Bessel function $j_l(\mu_{ln}r/R)$ and spherical harmonics $Y_{lm}(\theta,\varphi)$ become valid for the large root numbers $n\gg l\gg 1$ and small values of the angle θ:[30]

$$j_l(x)=\frac{1}{x}\sin\left(x-\frac{\pi l}{2}-\frac{\pi}{4}\right), \tag{32}$$

$$Y_{lm}(\theta,\varphi)=\sqrt{\frac{l}{2\pi}}e^{im\varphi}J_m(l\theta), \tag{33}$$

with $J_m(x)=\pi^{-1}\int_0^{\pi}\exp(ix\cos\phi)\cos(m\phi)d\phi$ being the Bessel function of order m.

Making use of Eqs. (32) and (33), the matrix elements present in Eq. (12) can be rewritten as

$$A_{js}=\begin{cases}(-1)^n\sqrt{\dfrac{l}{2\pi}}\langle\psi|\sin(k_z z)e^{i\mathbf{k}_{\parallel}\vec{\rho}_{\parallel}}|\psi\rangle=(-1)^n\sqrt{\dfrac{l}{2\pi}}F^{(1)}_{\mathbf{k}}, & j=1\\ \sqrt{\dfrac{l}{2\pi}}\langle\psi|e^{-k_{\parallel}z}e^{i\mathbf{k}_{\parallel}\vec{\rho}_{\parallel}}|\psi\rangle=\sqrt{\dfrac{l}{2\pi}}F^{(2)}_{\mathbf{k}_{\parallel}}, & j=2,\end{cases} \tag{34}$$

$$B_{js}=\begin{cases}\left(\sqrt{\dfrac{l}{2\pi}}\right)^2\langle\psi|\sin^2(k_z z)|\psi\rangle=\left(\sqrt{\dfrac{l}{2\pi}}\right)^2 G^{(1)}_{\mathbf{k}}, & j=1\\ \left(\sqrt{\dfrac{l}{2\pi}}\right)^2\langle\psi|e^{-2k_{\parallel}z}|\psi\rangle=\left(\sqrt{\dfrac{l}{2\pi}}\right)^2 G^{(2)}_{\mathbf{k}_{\parallel}}, & j=2,\end{cases} \tag{35}$$

$$C_{js}=\begin{cases}R_p^2\left(\sqrt{\dfrac{l}{2\pi}}\right)^2\langle\psi||\nabla(\sin(k_z z)e^{i\mathbf{k}_{\parallel}\vec{\rho}_{\parallel}})|^2|\psi\rangle=\left(\sqrt{\dfrac{l}{2\pi}}\right)^2 R_p^2 H^{(1)}_{\mathbf{k}}, & j=1,\\ R_p^2\left(\sqrt{\dfrac{l}{2\pi}}\right)^2\langle\psi||\nabla(e^{-k_{\parallel}z}e^{i\mathbf{k}_{\parallel}\vec{\rho}_{\parallel}})|^2|\psi\rangle=\left(\sqrt{\dfrac{l}{2\pi}}\right)^2 R_p^2 H^{(2)}_{\mathbf{k}_{\parallel}}, & j=2,\end{cases} \tag{36}$$

where $k_z=\pi n/R$, $\mathbf{k}_{\parallel}\vec{\rho}_{\parallel}=(l/R)\rho_{\parallel}\cos\phi$, $\rho_{\parallel}=\rho\sin\Theta$, and ϕ is the angle between vectors $\mathbf{k}_{\parallel}$ and $\vec{\rho}_{\parallel}$.

Substitution of these matrix elements in Eqs. (13) and (14), and replacement of the sums by the corresponding integrals, leads to the following expressions for the electron–bulk-phonon and electron–SO-phonon interaction energies:

$$E^{(b)}_{pol}=-\hbar\omega_{LO}\frac{4\alpha R_p}{\pi}\int_0^{\infty}\int_0^{\infty}\frac{dk_z dk_{\parallel}k_{\parallel}}{k_z^2+k_{\parallel}^2}\times\frac{G^{(1)}_{\mathbf{k}}(G^{(1)}_{\mathbf{k}}-F^{(1)}_{\mathbf{k}})+R_p^2(F^{(1)}_{\mathbf{k}})^2H^{(1)}_{\mathbf{k}}}{G^{(1)}_{\mathbf{k}}+R_p^2H^{(1)}_{\mathbf{k}}-(F^{(1)}_{\mathbf{k}})^2} \tag{37}$$

$$E^{(s)}_{pol}=-\hbar\omega_{LO}\frac{2\alpha R_p\varepsilon_0\varepsilon_{\infty}}{(\varepsilon_0+\varepsilon_d)(\varepsilon_{\infty}+\varepsilon_d)}\int_0^{\infty}dk_{\parallel}\times\frac{G^{(2)}_{\mathbf{k}_{\parallel}}(G^{(2)}_{\mathbf{k}_{\parallel}}-F^{(2)}_{\mathbf{k}_{\parallel}})+R_p^2(F^{(2)}_{\mathbf{k}_{\parallel}})^2H^{(2)}_{\mathbf{k}_{\parallel}}}{G^{(2)}_{\mathbf{k}_{\parallel}}+R_p^2H^{(2)}_{\mathbf{k}_{\parallel}}-(F^{(2)}_{\mathbf{k}_{\parallel}})^2}. \tag{38}$$

The equations above can be regarded as an extension of the method developed in Ref. 26 to the case of the surface polaron. Using them, the total polaron energy can be found by the standard minimization procedure for arbitrary values of the constant α and the electron-impurity interaction. However, since the detailed investigation of the surface polaron problem is beyond the scope of the present paper, we will

limit ourselves by considering only the limiting case of the bound surface polaron interacting weakly with phonons and an impurity, which gives some physical information pertinent to the bound polaron confined in a quantum dot.

In this case the relations $F_{\mathbf{k}}^{(1)} \ll G_{\mathbf{k}}^{(1)}$, $F_{\mathbf{k}_\parallel}^{(2)} \ll G_{\mathbf{k}_\parallel}^{(2)}$ and $H_{\mathbf{k}}^{(1)} = k^2 R_p^2 G_{\mathbf{k}}^{(1)}$, $H_{\mathbf{k}_\parallel}^{(2)} = 2k_\parallel^2 R_p^2 G_{\mathbf{k}_\parallel}^{(2)}$ hold. Thus, Eqs. (37) and (38) for large values of z ($z \gg R_p$) reduce to

$$E_{pol}^{(b)} = -\alpha\hbar\omega_{LO} + \left\langle \psi \left| \left(\frac{1}{\varepsilon_\infty} - \frac{1}{\varepsilon_0} \right) \frac{e^2}{4z} \right| \psi \right\rangle, \tag{39}$$

$$E_{pol}^{(s)} = \left\langle \psi \left| \left(\frac{\varepsilon_0 - \varepsilon_d}{\varepsilon_0 + \varepsilon_d} - \frac{\varepsilon_\infty - \varepsilon_d}{\varepsilon_\infty + \varepsilon_d} \right) \frac{e^2}{4\varepsilon_d z} \right| \psi \right\rangle, \tag{40}$$

which are the same as were obtained by Evans and Mills.[31] Combining them with the asymptotic values for the electrostatic energy and the electron-impurity exchange potential,

$$V_C(\vec{\rho}) = -\frac{1}{\varepsilon_\infty}\frac{e^2}{\rho} - \frac{\varepsilon_\infty - \varepsilon_d}{\varepsilon_\infty + \varepsilon_d}\frac{e^2}{\varepsilon_\infty \rho} + \frac{\varepsilon_\infty - \varepsilon_d}{\varepsilon_\infty + \varepsilon_d}\frac{e^2}{4\varepsilon_\infty z}, \tag{41}$$

$$H_x = \left(\frac{\varepsilon_0 - \varepsilon_d}{\varepsilon_0 + \varepsilon_d} - \frac{\varepsilon_\infty - \varepsilon_d}{\varepsilon_\infty + \varepsilon_d} \right) \frac{e^2}{4\varepsilon_d \rho}, \tag{42}$$

one obtains the polaron energy in the form

$$E = -\alpha\hbar\omega_{LO} - \langle \psi | \left[\frac{1}{(\varepsilon_0 + \varepsilon_d)/2} \frac{e^2}{\rho} - \frac{\varepsilon_0 - \varepsilon_d}{\varepsilon_0 + \varepsilon_d} \frac{e^2}{4\varepsilon_d z} \right] | \psi \rangle. \tag{43}$$

From this equation the physical meaning of all terms is seen: from the two image charge terms present in the electrostatic energy V_C, one is responsible for the interaction of the impurity with its image (the second term) while the other corresponds to the interaction of the electron with its image (the third term). The presence of the exchange potential H_x arising from the impurity-phonon interaction gives rise to the renormalization of the second term in the electrostatic energy (ε_∞ is replaced by ε_0) much like the case of the bound bulk polaron.[32] The electron-phonon interaction ($E_{pol}^{(s)}$ and the second part of $E_{pol}^{(b)}$) produces the same result for the electronic part of V_C, making the net effect like that from the classical electrostatic potential. The first part of $E_{pol}^{(b)}$ shifts the bottom of the conduction band analogously to the case of the bulk bound polaron. It should also be noted that this effect occurs only when the electron is weakly localized around the impurity, so that the binding energy of the electron and its interaction with phonons are small, and is quite similar to the results of Ref. 31. Thus we see that the interaction of the electron with surface phonons is not responsible for the creation of the image charge potential (except for the trivial case when $\varepsilon_\infty = \varepsilon_d$); it just gives rise to its renormalization, and it is important to treat the image charge effects properly since they should significantly affect the total polaron energy for all values of the binding and coupling.

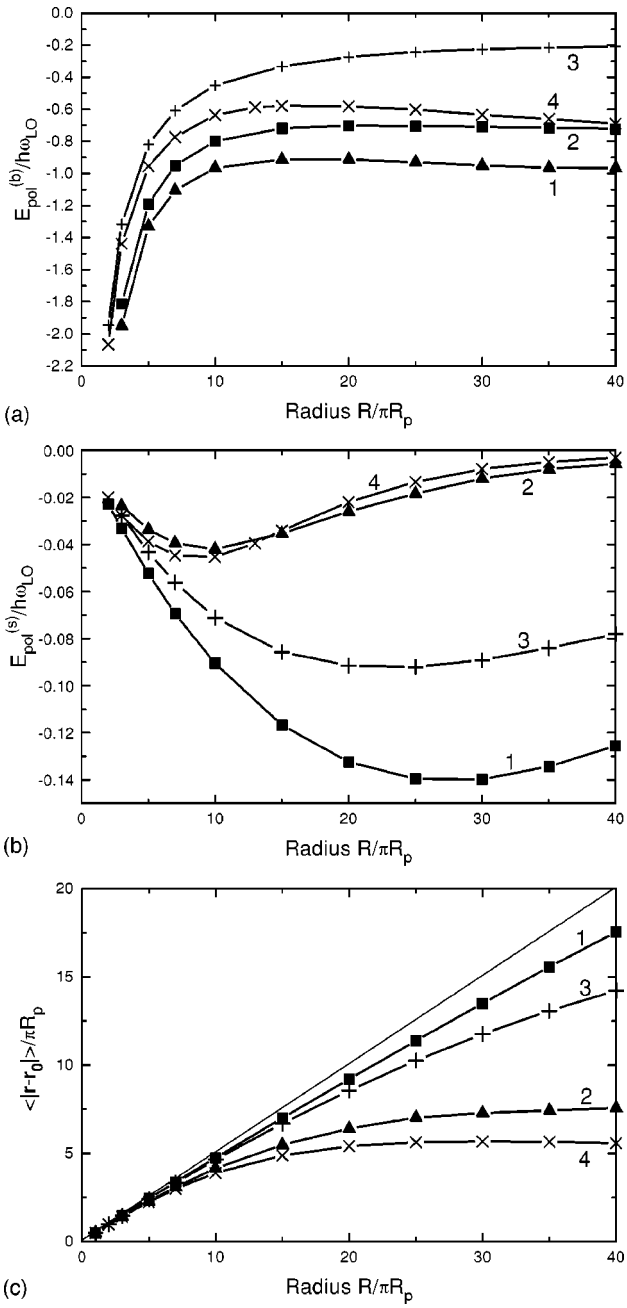

FIG. 1. (a) Dependence of the electron–bulk-phonon interaction energy $E_{pol}^{(b)}$ on the radius of the quantum dot R ($r_0 = 0$): curve 1 corresponds to a system with $\alpha = 1$, $\varepsilon_\infty/\varepsilon_0 = 0.1$; curve 2 to a system with $\alpha = 1$, $\varepsilon_\infty/\varepsilon_0 = 0.5$; curve 3 to a system with $\alpha = 6$, $\varepsilon_\infty/\varepsilon_0 = 0.1$; and curve 4 to a system with $\alpha = 6$, $\varepsilon_\infty/\varepsilon_0 = 0.5$. All other parameters are given in the text. Results for curves 3 and 4 are divided by 20 and 50, respectively, to fit the scale of the graph; the scaling factor on the horizontal axis is 0.05 for curves 1 and 2 and 0.01 for curves 3 and 4. Dots represent calculated values, and the curves are a guide to the eye. (b) Dependence of the electron–SO-phonon interaction energy $E_{pol}^{(s)}$ on the radius of the quantum dot R: all curves are calculated using the same values of parameters as in (a). (c) Dependence of the average electron-impurity distance $\langle|\mathbf{r} - \mathbf{r_0}|\rangle$ on the radius of the quantum dot R: the scaling factor is equal to 0.05 for curves 1 and 2 and to 0.01 for curves 3 and 4; all curves are calculated using the same values of parameters as in (a).

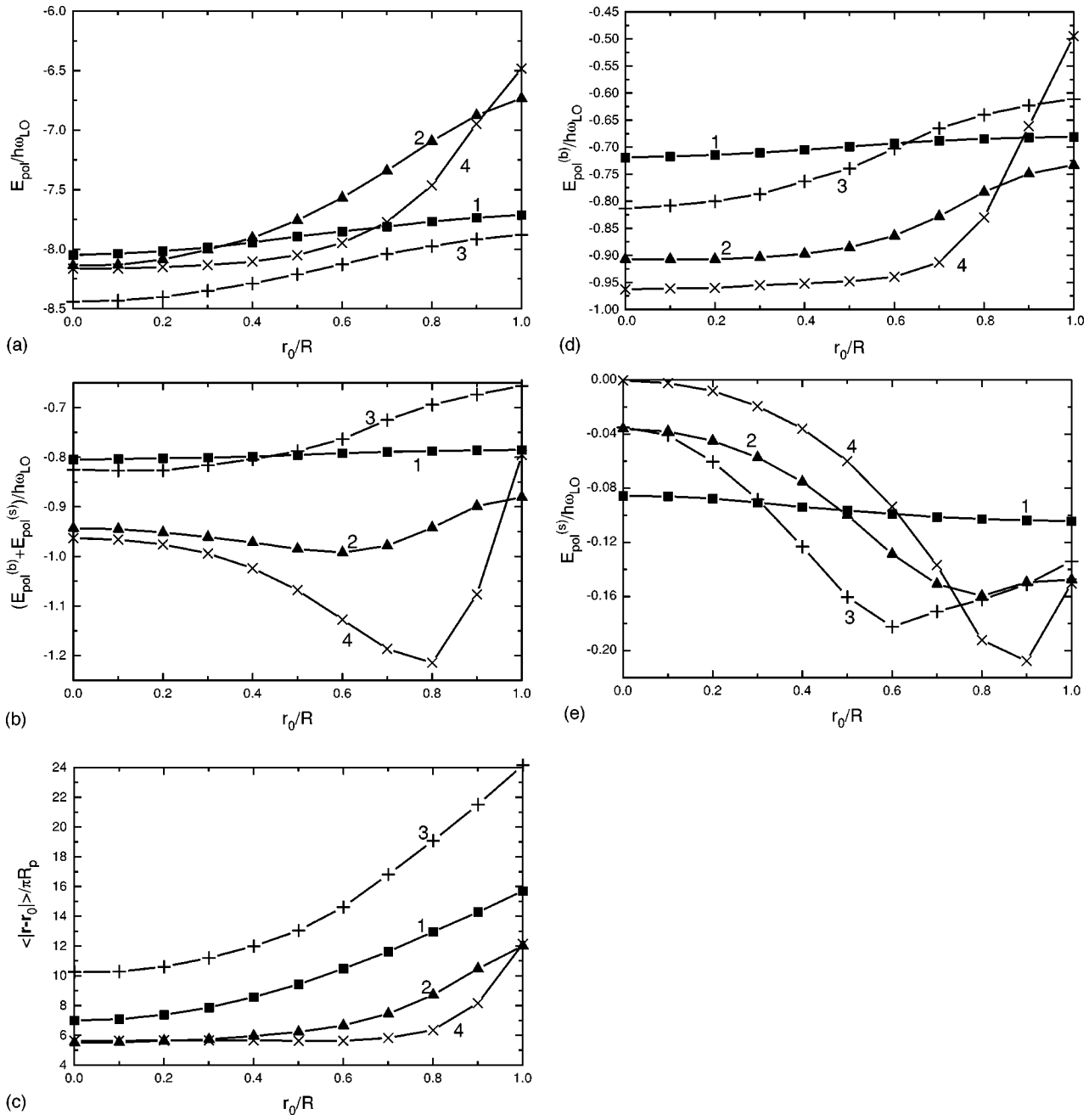

FIG. 2. (a) The polaron energy E_{pol} as a function of the impurity position r_0/R for a QD with $R/\pi R_p=0.75$ for curves 1 and 2, and $R/\pi R_p=0.25$ for others. Results for curve 1 are multiplied by 2; results for curves 3 and 4 are divided by 8 and 20, respectively, to fit the scale of the graph; the values of the parameters are the same as in Fig. 1(a). (b) The total electron-phonon interaction energy as a function of the impurity position; curves 3 and 4 are scaled down by 12 and 25 times to fit the graph; the parameters specifying different curves are the same as for Fig. 1(a). (c) The average electron-impurity distance $\langle|\mathbf{r}-\mathbf{r_0}|\rangle$ as a function of the impurity position; the parameters specifying different curves are the same as for Fig. 1(d). (d) The electron–bulk-phonon interaction energy as a function of the impurity position; curves 3 and 4 are scaled down by 12 and 25 times to fit the graph; the parameters specifying different curves are the same as for Fig. 1(a). (e) The electron–SO-phonon interaction energy as a function of the impurity position; curves 3 and 4 are scaled down by four and 50 times respectively, the parameters specifying different curves are the same as for Fig. 1(a).

IV. RESULTS OF NUMERICAL CALCULATIONS

Now, changing physical parameters of the system, we calculate the polaron energy and systematically discuss the general properties of the bound polaron confined in a spherical quantum dot. The present system is characterized by the following physical parameters: the electron effective mass m, the static and high-frequency dielectric constants ε_0 and ε_∞ of the material inside the QD, the dielectric constant of the surrounding matrix ε_d, the bulk LO-phonon energy of the dot material $\hbar\omega_{LO}$, the radius of the QD R, and the position of the impurity inside the quantum dot r_0. Values of some these parameters are given in Table I. If we take the polaron

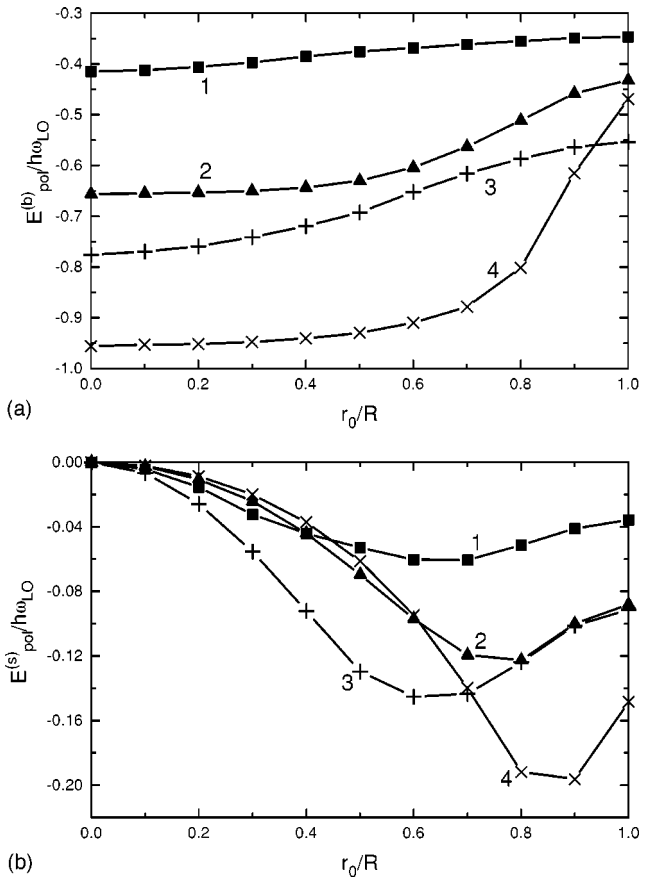

FIG. 3. (a) The electron–bulk-phonon interaction energy in the adiabatic case as a function of the impurity position; curves 3 and 4 are scaled down by 12 and 25 times to fit the graph; the parameters specifying different curves are the same as for Fig. 1(a). (b) The electron–SO-phonon interaction energy in the adiabatic case as a function of the impurity position; curve 1 is multiplied by 10, curves 3 and 4 are scaled down by 4 and 50 times respectively, and the parameters specifying different curves are the same as for Fig. 1(a).

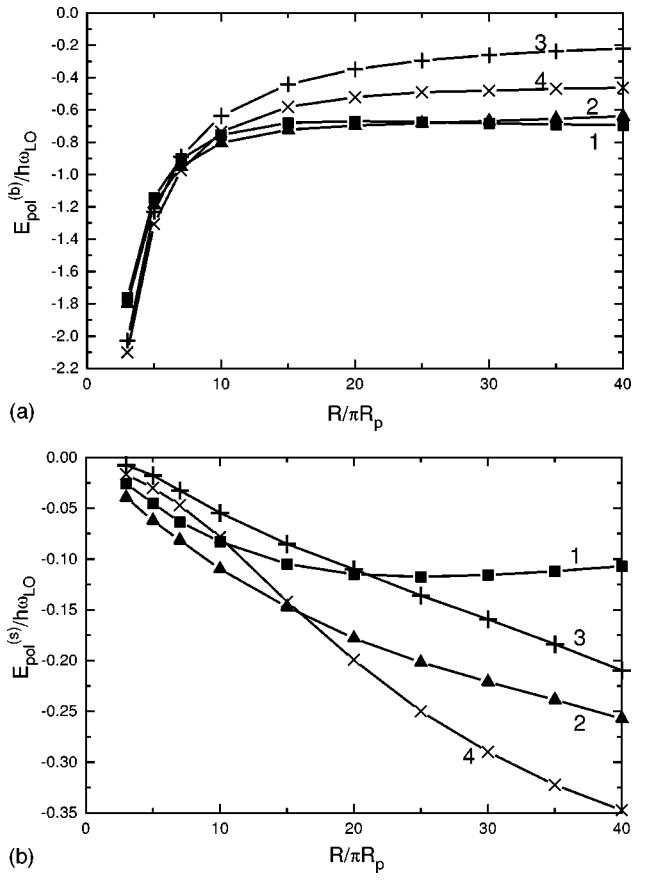

FIG. 4. (a) Dependence of the the electron–bulk-phonon interaction energy $E^{(b)}_{pol}$ on the radius of the quantum dot for the case of the impurity on the surface ($r_0/R=1$); curves 3 and 4 are scaled down by a factor of 25, and all curves are calculated using the same values of parameters as in Fig. 1(a). (b) Dependence of the electron–SO-phonon interaction energy $E^{(s)}_{pol}$ on the radius of the quantum dot; curves 3 and 4 are scaled down by a factor of 4 and 30, respectively, and all curves are calculated using the same values of parameters as in Fig. 1(a).

radius R_p and $\hbar\omega_{LO}$ as units of length and energy, then the properties of the system can be characterized by the following five parameters: the electron-phonon coupling strength α [see Eq. (12)], the electron-impurity binding strength $\varepsilon_\infty/\varepsilon_0$,[33] the effect of the image charge potential $\varepsilon_d/\varepsilon_0$, the size of the QD R/R_p, and the impurity position r_0/R. To discuss the general properties of the electron-phonon interaction in the QD, these quantities will be varied in a wide range covering the interval of the real material parameters given by Table I.

The results of the numerical calculations for the polaron energy, contributions from the electron–bulk-phonon and electron–SO-phonon interactions for various impurity positions and dot radii are first given here for two values of the coupling parameter $\alpha=1$ and 6, keeping the fixed value of $\varepsilon_d/\varepsilon_0=0.164$. For each of the electron-phonon coupling constants two values of the ratio $\varepsilon_\infty/\varepsilon_0$ are chosen, $\varepsilon_\infty/\varepsilon_0=0.1$ and 0.5, corresponding to weak and strong bindings, respectively. After this the effect of the surrounding material is studied separately for different QD's, changing the ratio of $\varepsilon_d/\varepsilon_0$ but keeping other material parameters fixed ($\alpha=1$, $\varepsilon_\infty/\varepsilon_0=0.5$).

First the dependence of the electron–bulk-phonon interaction energy on the radius of the quantum dot for the case of $r_0=0$ is plotted in Fig. 1(a). The absolute value of this energy increases rapidly as the dot's radius becomes small, in agreement with results of Sec. III. It is also seen that the magnitude of this energy is greater for stronger binding and coupling. It is also visible from the curves shown in this figure that the magnitude of the electron–bulk-phonon energy decreases rapidly from a large value as the radius of the dot increases, passes through a minimum, and then gradually approaches the bulk value. The presence of this minimum is due to the nonadiabatic processes whose roles become more important as the radius increases. The interaction with SO phonons also exhibits a minimum at some intermediate radius, but this time as $R\to 0$ and $R\to\infty$ this energy approaches zero [see Fig. 1(b)]. Also note that the increase of binding and coupling strengths results in a decrease of this energy magnitude, since the electron becomes more localized

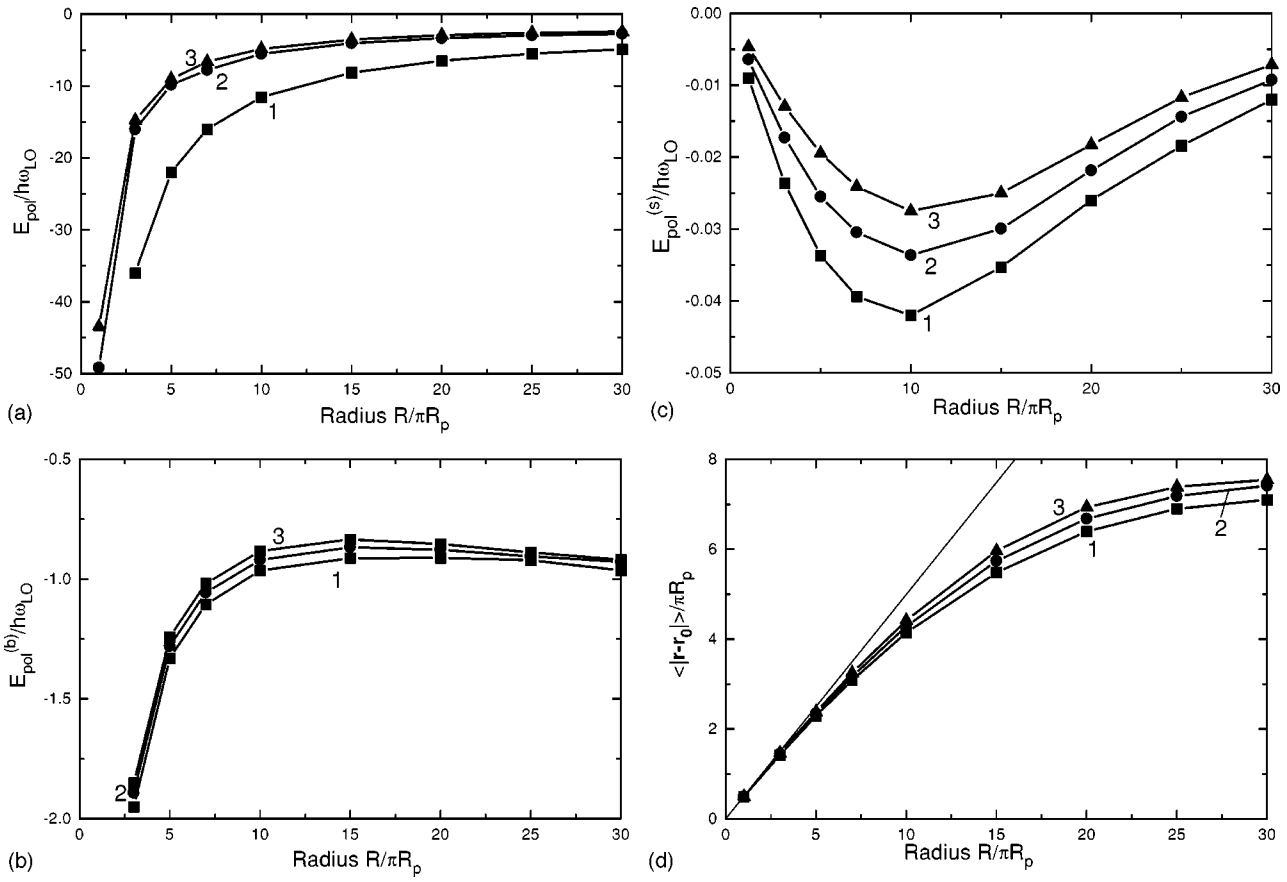

FIG. 5. (a) Dependence of the polaron energy E_{pol} on the radius of the quantum dot for $r_0=0$: curve 1 corresponds to a system with $\varepsilon_d/\varepsilon_\infty=0.164$, curve 2 to a system with $\varepsilon_d/\varepsilon_\infty=1$, and curve 3 to a system with $\varepsilon_d/\varepsilon_\infty=5$. The scaling factor for the horizontal axis is 0.05. All other parameters are defined in the text. (b) Dependence of the electron-bulk-phonon interaction energy $E_{pol}^{(b)}$ on the radius of the quantum dot R; all curves are calculated using the same values of parameters as in Fig. 4(a). (c) Dependence of the electron–SO-phonon interaction energy $E_{pol}^{(s)}$ on the radius of the quantum dot R; results for curves 2 and 3 are multiplied by 3 and 25, respectively, and all curves are calculated using the same values of parameters as in Fig. 4(a). (d) Dependence of the average electron-impurity distance $\langle|\mathbf{r}-\mathbf{r_0}|\rangle$ on the radius of the quantum dot R: the scaling factor is 0.05, and all curves are calculated using the same values of parameters as in Fig. 4(a).

around the impurity and thus effectively farther from the surface. The effect of the increase in electron localization is also quite visible on the plots of the average electron-impurity distance $\langle|\mathbf{r}-\mathbf{r_0}|\rangle$ presented in Fig. 1(c): in the limit of $\gamma=0$ (no impurity and interaction with phonons) this value should be equal to $R/2$ shown as a straight line in Fig. 1(c), while the stronger the binding and/or coupling, the greater the deviation of the curves from the line $\langle|\mathbf{r}-\mathbf{r_0}|\rangle = R/2$ is observed.

To see how the different impurity positions affect the results, we plotted the same quantities as above, but as a function of the impurity position r_0/R. The polaron energy as well as the average electron-impurity position have minima at $r_0=0$ for all studied values of binding and coupling as seen in Figs. 2(a) and 2(c), and then they increase as the impurity is moved away from the center and reach their maxima at $r_0/R=1$. This would correspond to a gradual transition from the $1s$ state to the $2p$ state for a very large quantum dot, as shown in Sec. III. It should also be mentioned that the stronger binding with a fixed electron-phonon coupling value causes larger variations in the energy as the position r_0 is changed. The total value of the electron-phonon interaction (bulk and SO modes) has a maximum in magnitude when the impurity is positioned in the center of the dot for the weak coupling and binding [Fig. 2(b), curve 1], and reaches its maximum at some intermediate value of r_0 for greater values of α and $\varepsilon_\infty/\varepsilon_0$.

In order to clarify this qualitative change, the dependencies of the electron–bulk-phonon $E_{pol}^{(b)}$ and electron–surface-phonon $E_{pol}^{(s)}$ interaction energies are plotted separately in Figs. 2(d) and 2(e). The quantity $E_{pol}^{(b)}$ has a minimum for $r_0=0$, and increases gradually to its maximum for $r_0/R=1$. The lower value of the ratio $\varepsilon_\infty/\varepsilon_0$ corresponds to the weaker dependence of this energy on the impurity position. The electron–SO-phonon interaction energy changes its value by an order of magnitude with the increase of coupling from $\alpha=1$ to 6 when $\varepsilon_\infty/\varepsilon_0=0.5$. Its dependence on r_0 is also stronger for $\alpha=6$ and $\varepsilon_\infty/\varepsilon_0=0.5$. When $r_0=0$, the magnitude of $E_{pol}^{(s)}$ has a minimum, and increases significantly as the impurity is shifted toward the surface. However, it reaches its maximun on the surface only for weak coupling and binding, while for the rest of the studied parameters the maximum value occurs when the impurity is inside the dot

but close to the surface. This considerable increase in the electron–SO-phonon interaction is responsible for the minimum in the total electron-phonon energy when the impurity is positioned away from the center of the dot. The qualitative change in the energy vs impurity position behavior can be attributed to the transition from the weak-coupling approach to the adiabatic case, which governs the situation for stronger binding or coupling cases in the confined systems such as the spherical QD considered here. Note that in the bulk $\alpha=6$ corresponds to the intermediate-coupling case while in the case of the QD system the behavior of the interaction energies agrees qualitatively with the predictions of the adiabatic approach.

To prove this point, we have also performed calculations of the electron-phonon interaction energy for the same set of parameters, but using the adiabatic variational approach using only the first terms in brackets in Eqs. (13) and (14). The results for the electron–bulk-phonon and electron–SO-phonon interactions as functions of the impurity position r_0 are presented in Figs. 3(a) and 3(b), respectively. Comparison with the corresponding curves in Figs. 2(d) and 2(e) shows that in general the adiabatic approach underestimates the value of the electron-phonon interaction energy, especially for weak coupling and/or binding [cf. curve 1 in Figs. 2(d) and 2(e) and 3(a) and 3(b)]. As the value of the coupling and/or binding increases, the results of the full all-coupling and adiabatic methods approach each other [cf., e.g., curve 4 in Figs. 2(d) and 2(e) and 3(a) and 3(b)]. It is also seen that the behavior of the electron–SO-phonon interaction obtained by these two methods is rather different: when the impurity is positioned in the center of the dot, $E_{pol}^{(s)}$ is equal to zero for the adiabatic approach and has a nonzero value in the all-coupling case, in agreement with predictions of Sec. III A. When the impurity is located close to the surface of the dot, this interaction energy reaches a maximum in absolute value inside the dot in the adiabatic case for all values of the coupling and binding, but only for sufficiently strong coupling and binding in the all-coupling method [cf. curve 1 in Figs. 2(e) and 3(b)]. This can be attributed to the fact that the adiabatic method enhances the localization of the electron around the impurity compared to the all-coupling method (see, e.g, Sec. III A) and thus effectively decreases the electron–SO-phonon interaction when the adiabatic case is applied to the systems with weak electron-phonon and electron-impurity interactions.

The significant decrease in the values of the electron–SO-phonon interaction energies for the case of the impurity located on the dot's surface is clearly seen in the results given in Fig. 4(a). Unlike the dependencies from Fig. 1(b), the magnitude of this interaction energy is much larger for a stronger binding and coupling, and amounts to up to 50% of the electron–bulk-phonon energy for sufficiently large QD radii [cf. Figs. 4(a) and 4(b)]. This can be explained by noting that the increase in the coupling and/or binding enhances the electron localization around the impurity, thus forcing the electron to interact strongly with SO phonons. This result is quite different from those obtained for the free polaron confined in the QDs (see, e.g, Ref. 7) since in that case the electron is always spread across the dot and the increase of the electron-phonon coupling gives rise to an increase of the electron localization in the center of the dot, making it farther from the dot's surface and diminishing its interaction with SO phonons. In our case, the electron is always localized around the impurity, and moves away from the center of

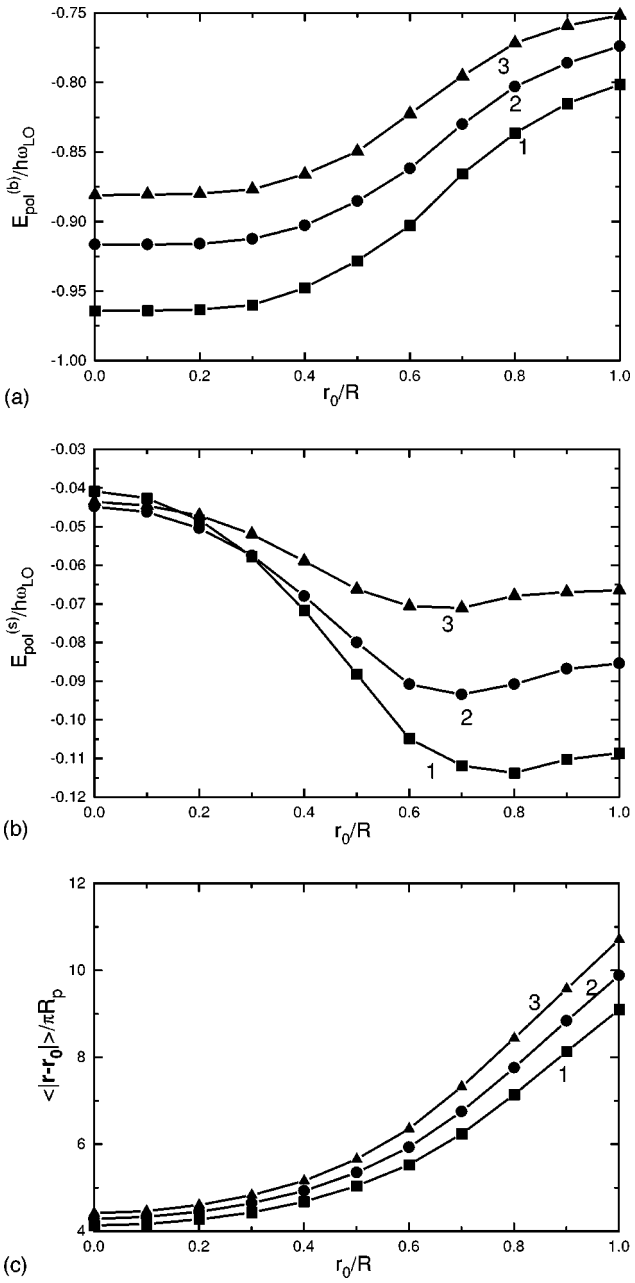

FIG. 6. (a) The electron–bulk-phonon interaction energy as a function of the impurity position r_0/R for a QD with $R/\pi R_p = 0.5$; the values of parameters are the same as in Fig. 4(a). (b) The electron–SO-phonon interaction energy as a function of the impurity position; the results for curves 2 and 3 are multiplied by 4 and 40, respectively, all other parameters specifying different curves are the same as for Fig. 4(a). (c) The average electron-impurity distance $\langle|\mathbf{r}-\mathbf{r_0}|\rangle$ as a function of the impurity position; the scaling factor is 0.05, and other parameters specifying different curves are the same as for Fig. 4(a).

the dot as the impurity is shifted toward the surface of the quantum dot.

Now let us consider the effect of the image charge potential on the electron-phonon interaction. The study of this effect is provided for three values of the ratio $\varepsilon_d/\varepsilon_\infty=0.164$, 1, and 5 keeping the electron-phonon coupling constant α equal to unity and the parameter $\varepsilon_\infty/\varepsilon_0=0.5$. Note that the situation $\varepsilon_d/\varepsilon_\infty=1$ corresponds to the absence of the image potential contribution to the total energy. From Fig. 5(a) (the impurity is in the center of the dot), one can see that small values of the matrix dielectric constant ε_d result in a notable decrease of the total polaron energy compared to the situation when $\varepsilon_d/\varepsilon_\infty=1$ and 5. This can be understood by realizing that for small values of the dielectric constant ratio the leading term of the image potential becomes $-e^2/2\varepsilon_d R$, causing this significant change in the value of the polaron energy analogously to the results obtained for quantum-well systems.[34] However, these changes in the total energy do not affect the electron–bulk-phonon interaction energy, as can be seen from the data presented in Fig. 5(b). The interaction energy between the electron and SO phonons given in Fig. 5(c), conversely changes drastically with the increase of the ε_d value, since this energy depends on it as ε_d^{-2}. The radius of the electron localization is also weakly dependent on the value of the image potential, as seen in Fig. 5(d).

The dependencies in Fig. 6 on r_0/R with fixed value of R show the electron–bulk-phonon interaction energy [Fig. 5(a)] and the value of the average electron-impurity distance [Fig. 5(c)]; it just shifts these quantities as a whole along the energy axis, and this shift is significant for the total polaron energy but rather small for the electron-phonon contribution and average distance dependencies. On the other hand, the electron–SO-phonon interaction depends strongly on the strength of the image potential as can be observed from the curves plotted in Fig. 5(b): the stronger the potential (the greater the ratio $\varepsilon_d/\varepsilon_\infty$), the smaller the dependence of this energy on the impurity position, which can be explained by the fact that in this case the image charge potential is divergent as $(R-r)^{-1}$ for most values of $\mathbf{r}/r$ when $r\to R$. This potential repels the electron away from the surface, effectively decreasing its interaction with surface phonons.

V. CONCLUDING REMARKS

The effect of the electron interaction with LO phonons was discussed for an electron bound to a hydrogenlike impurity perfectly confined in a spherical quantum dot embedded in a nonpolar matrix. Both bulk and SO phonons were taken into account when calculating the energy of the polaron. An all-coupling variational method appropriate for the description of the polaron effects in a broad range of the QD sizes and material parameters was used. Using this method, the limiting cases of small QD's (adiabatic approach) and large QD's were first studied, and some general analytical results were obtained. It was shown that in the large dot limit this method transforms into the standard variational approach used in the bulk and surface polaron models, and its implications were studied for the cases of the impurity located in the center and on the surface of the dot which would correspond to the $1s$ and $2p$ states of the bare electron.

Results of the numerical simulations show that for any value of coupling and for small binding strength the total electron-phonon interaction energy depends weakly on the impurity position, and has a maximum when the impurity is at the center of the dot. As the binding strength increases, the maximum of the electron-phonon interaction energy shifts inside the dot. The interaction with bulk and SO phonons is greater for the stronger electron-impurity interaction case provided the value of the electron-phonon coupling stays the same and the impurity is close to the surface. This interaction can be quite significant, and comparable to the electron–bulk-phonon interaction energy for strong coupling and binding. As the impurity position is changed, the maximum (in absolute value) of this energy occurs on the surface of the dot in the weak coupling or binding regime, unlike the results obtained in the adiabatic limit, and shifts inside the QD with the increase of the coupling-binding strength and/or electron-impurity binding, contrary to the situation observed in the quantum-well structures.[35] The image charge potential gives rise to a significant lowering of the total polaron energy when the dielectric constant of the matrix is smaller than the high-frequency dielectric constant of the QD material, and it increases the polaron energy in the opposite limit.

To conclude, we mention one of the possible future extensions of this work. This concerns the more realistic case of imperfect electron confinement in a QD (finite value potential barrier on the interface), which should also be studied taking into account the frequent situation when the LO phonons are present not only in the dot but also within the barrier (such as CuCl in a NaCl crystal) where it is expected that the all-coupling variational method will work well. However, the Hamiltonian used in this paper is, strictly speaking, valid only for the infinite values of the surface potential barrier when the dot is embedded in the matrix; this is manifested in the form of the electron–bulk-phonon interaction potentials and in the choice of the electron trial function. Therefore, in order to attempt such a study, certain changes should first be done to the initial Hamiltonian of the problem. Only after that can an accurate comparison with available experimental data be made.

ACKNOWLEDGMENTS

We would like to thank F. Ham, M. Stavola, M. White, and R. Folk for useful discussions of these results. One of the authors (D.V.M.) also acknowledges support in the form of a Sherman Fairchild Fellowship.

[1] A.D. Ioffe, Adv. Phys. **42**, 173 (1993).
[2] U. Woggon and S.V. Gaponenko, Phys. Status Solidi B **189**, 285 (1995).
[3] R. Englman and R. Ruppin, J. Phys. C **1**, 614 (1968).
[4] J.S. Pan and H.B. Pan, Phys. Solid State **148**, 129 (1988).
[5] M.C. Klein, F. Hache, D. Ricard, and C. Flytzanis, Phys. Rev. B **42**, 11123 (1990).
[6] J.C. Marini, B. Strebe, and E. Kartheuser, Phys. Rev. B **50**, 14302 (1994).
[7] K. Oshiro, K. Akai, and M. Matsuura, Phys. Rev. B **58**, 7986 (1998).
[8] W.S. Lee and C.Y. Chen, Physica B **229**, 375 (1997).
[9] R.M. Cruz, Superlattices Microstruct. **17**, 307 (1995).
[10] M.H. Degani and H.A. Farias, Phys. Rev. B **42**, 11950 (1990).
[11] K.-D. Zhu and S.-W. Gu, Phys. Lett. A **58**, 435 (1992).
[12] S. Mukhopadhyay and A. Chatterjee, Phys. Rev. B **55**, 9279 (1997).
[13] E.P. Pokatilov, V.M. Fomin, J.T. Devreese, S.N. Balaban, and S.N. Klimin, Physica E **4**, 156 (1999).
[14] S.N. Klimin, E.P. Pokatilov, and V.M. Fomin, Phys. Status Solidi B **184**, 373 (1994).
[15] A. Uhrig, L. Banyai, Y.Z. Hu, S.W. Koch, C. Klingshirn, and N. Neuroth, Z. Phys. B: Condens. Matter **81**, 385 (1990); A. Uhrig, L. Banyai, S. Gaponenko, A. Worner, N. Neuroth, and C. Klingshirn, Z. Phys. D: At., Mol. Clusters **20**, 345 (1991).
[16] M. Bissiri, G. Baldassarri, Höger von Högersthal, A.S. Bhatti, M. Capizzi, A. Frova, P. Frigeri, and S. Franchi, Phys. Rev. B **62**, 4642 (2000).
[17] T.K. Mitra, Phys. Rep. **153**, 93 (1987).
[18] H. Vogelsang, O. Husberg, U. Köhler, W. von der Osten, and A.P. Marchetti, Phys. Rev. B **61**, 1847 (2000).
[19] A.I. Ekimov, I.A. Kudravtsev, M.G. Ivanov, and Al.L. Efros, J. Lumin. **46**, 83 (1990).
[20] N. Porras-Montenegro and S.T. Perez-Merchancano, Phys. Rev. B **46**, 9780 (1992).
[21] J.-L. Zhu and X. Chen, Phys. Rev. B **50**, 4497 (1994).
[22] H.-J. Xie and C.-Y. Chen, Eur. Phys. J.: Appl. Phys. **5**, 215 (1998).
[23] D.V. Melnikov and W.B. Fowler, Phys. Rev. B **63**, 165302 (2001).
[24] *Semiconductors-Basic Data*, edited by O. Madelung (Springer, New York, 1996).
[25] S.A. McGill, K. Cao, W.B. Fowler, and G.G. DeLeo, Phys. Rev. B **57**, 8951 (1998).
[26] M. Matsuura and H. Büttner, Phys. Rev. B **21**, 679 (1980).
[27] J. Adamowski, Phys. Rev. B **32**, 2588 (1985).
[28] J. Devreese, R. Evrard, E. Kartheuser, and F. Brosens, Solid State Commun. **44**, 1435 (1982).
[29] J.D. Levine, Phys. Rev. **A140**, 586 (1965).
[30] M. Abramowitz and I. Stegun, *Handbook of Mathematical Functions* (Dover, New York, 1972); D. A. Varshalovich, A. N. Moskalev, and V. K. Khersonskii, *Quantum Theory of Angular Momentum* (World Scientific, Singapore, 1988).
[31] J. Sak, Phys. Rev. B **6**, 3981 (1972); E. Evans and D.L. Mills, *ibid.* **8**, 4004 (1973); R.-S. Zheng, S.-W. Gu, and D.L. Lin, Solid State Commun. **59**, 331 (1986).
[32] P.M. Platzman, Phys. Rev. **125**, 1961 (1962).
[33] It should be remarked that in the bulk polaron case the effect of the impurity binding is usually handled by changing the value of the Rydberg, since the exchange potential gives rise to the replacement $\varepsilon_\infty \rightarrow \varepsilon_0$; together with the value of α, these two parameters describe the bound polaron problem completely. In the case of QD's the exchange potential does not provide the full renormalization as in the bulk, and it is necessary to specify another independent parameter in addition to α to treat the problem in general.
[34] E.P. Pokatilov, S.I. Beril, V.M. Fomin, and V.V. Kalinovskii, Phys. Status Solidi B **161**, 603 (1990); S.I. Beril, E.P. Pokatilov, A.S. Zotov, and S. Madkur, *ibid.* **166**, 145 (1991); R. Zheng, and M. Matsuura, Phys. Rev. B **58**, 10769 (1998).
[35] Z.J. Shen, X.Z. Yuan, G.T. Shen, and B.C. Yang, Phys. Rev. B **49**, 11035 (1994).